PHILOSOPHICAL TRANSACTIONS OF THE ROYAL SOCIETY A MATHEMATICAL, PHYSICAL & ENGINEERING SCIENCES

Water availability in +2°C and +4°C worlds

Fai Fung, Ana Lopez and Mark New

Phil. Trans. R. Soc. A 2011 **369**, 99-116
doi: 10.1098/rsta.2010.0293

PHILOSOPHICAL TRANSACTIONS OF THE ROYAL SOCIETY A

Phil. Trans. R. Soc. A (2011) **369**, 99–116
doi:10.1098/rsta.2010.0293

Water availability in +2°C and +4°C worlds

By Fai Fung[1,*], Ana Lopez[2,1] and Mark New[1]

[1] *Tyndall Centre for Climate Change Research, School of Geography and the Environment, University of Oxford, South Parks Road, Oxford OX1 3QY, UK*
[2] *Centre for Climate Change Economics and Policy, London School of Economics and Political Science, Houghton Street, London WC2A 2AE, UK*

While the parties to the UNFCCC agreed in the December 2009 Copenhagen Accord that a 2°C global warming over pre-industrial levels should be avoided, current commitments on greenhouse gas emissions reductions from these same parties will lead to a 50 : 50 chance of warming greater than 3.5°C. Here, we evaluate the differences in impacts and adaptation issues for water resources in worlds corresponding to the policy objective (+2°C) and possible reality (+4°C). We simulate the differences in impacts on surface run-off and water resource availability using a global hydrological model driven by ensembles of climate models with global temperature increases of 2°C and 4°C. We combine these with UN-based population growth scenarios to explore the relative importance of population change and climate change for water availability. We find that the projected changes in global surface run-off from the ensemble show an increase in spatial coherence and magnitude for a +4°C world compared with a +2°C one. In a +2°C world, population growth in most large river basins tends to override climate change as a driver of water stress, while in a +4°C world, climate change becomes more dominant, even compensating for population effects where climate change increases run-off. However, in some basins where climate change has positive effects, the seasonality of surface run-off becomes increasingly amplified in a +4°C climate.

Keywords: climate change impacts; global water resources; water resources stresses; macro-scale hydrological model; ensembles; uncertainty

1. Introduction

In December 2009, the Copenhagen Accord [1] reiterated the need to restrict global warming to no more than 2°C above pre-industrial levels. Since the accord, pledges for greenhouse gas emissions reductions put forward by nations (which include all major greenhouse gas emitters) lead to a 50 : 50 chance of a peak global warming of at least 3°C above pre-industrial levels [2], with some estimates of the 50 : 50 warming as large as 3.9°C [3]. These commitments are clearly far below what is required to keep below the 2°C target with any reasonable probability, and even more so for a limit of 1.5°C, a possible long-term goal of the Copenhagen

*Author for correspondence (fai.fung@ouce.ox.ac.uk).

One contribution of 13 to a Theme Issue 'Four degrees and beyond: the potential for a global temperature increase of four degrees and its implications'.

Accord. Clearly, while 2°C remains an important policy target, larger warming is highly likely, and it is important to evaluate the difference in impact of warming between a world that meets its policy objective and one where there is significant overshoot of this target.

A large number of studies have assessed the impact of climate change on global water resources and have been reported in the series of assessment reports conducted by the Intergovernmental Panel on Climate Change (IPCC) [4] and in a number of other publications [5–11]. These analyses have typically used ensembles of global climate models (GCMs) developed by a number of modelling centres across the globe, the so-called ensembles of opportunity or multi-model ensembles (MMEs). These evaluations have assessed the time-evolving impacts under different emissions scenarios and the uncertainty that arises in future projections owing to different GCM structures [12,13], rather than the impacts that occur at particular global temperature change thresholds.

In this paper, we contrast water availability and water stress in a world where warming is limited to 2°C and one where policy fails and warming reaches 4°C. We make use of a new GCM dataset, from the ClimatePrediction.net (CPDN) experiment [14], in combination with data from the World Climate Research Programme's Coupled Model Intercomparison Project Phase 3 (CMIP3) multi-GCM archive [15]. These provide us with a wide range of realizations of a world that warms by 4°C, enabling us to identify differences in climate, surface run-off and population that determine water stress in '+2°C' and '+4°C' worlds. We begin the paper by introducing the climate and hydrological models used, and how the data are processed to define the +2°C and +4°C worlds. This is followed by a description of the scenarios of future population growth we developed and how these are used to define water stress. We then present results showing differences in water availability and stress in +0°C (present day), +2°C and +4°C worlds. Finally, the implications for global and regional water resources are discussed.

2. Models and data

(*a*) *The climate models*

The CPDN perturbed-physics ensemble (PPE; available from www.climateprediction.net) comprises a large number of runs of a state-of-the-art GCM, HADCM3L. This is a version of the UK Met Office's (UKMO) Unified Model comprising a 3.75° longitude by 2.5° latitude resolution atmospheric model coupled to an ocean model with the same resolution; this is a lower spatial resolution than the ocean model (1.25° longitude by 1.25° latitude) used in the UKMO's standard version of this model, HadCM3. Each individual run uses a configuration of the GCM, with parameters representing various physical processes set to different values within their acceptable range, as defined by the experts in the relevant parametrization scheme [16,17]; see www.climateprediction.net for more details. For each combination of parameter values, an initial condition ensemble is used, enabling separation of internal and parameter variability. PPEs provide an approach for exploring a wide range of future climates, and this information can be used to assess potential impacts of climate change under that range of plausible futures.

For this study, we have selected a subset of 1557 GCM runs from the CPDN experiment that provides global climate data from 1930 to 2079. This subset has been driven by the SRES A1B greenhouse gas emissions scenario, a 'middle of the road' scenario, representing a world in the twenty-first century with very rapid economic growth, rapid introduction of new and more efficient technologies and a world that does not rely too heavily on one particular energy source; total CO_2 emissions increase to just over 16 Gt carbon in the 2050s, and then decline slowly to 13.5 Gt by 2100 [18].

We also use an MME of 22 GCMs from the CMIP3 multi-model dataset [15] that have completed at least one model run forced by the SRES A1B scenario, and have archived precipitation and temperature for the period 1961–2079. This enables us to compare the hydrological response across different sources of uncertainty: parameter uncertainty in the case of the PPE, and combined parameter and structural uncertainty in the MME. The climate models used in this analysis include BCCR-BCM2.0, CGCM3.1, CNRM-CM3, CSIRO-MK3.5, CSIRO-MK3.0, GFDL-CM2.0, GFDL-CM2.1, GISS-AOM, GISS-EH, GISS-ER, FGOALS-g1.0, INGV-ECHAM4, INM-CM3.0, IPSL-CM4, MIROC3.2 (hires), ECHO-G, ECHAM5/MPI-OM, CCSM3, PCM, MRI-CGCM2.3.2, UKMO-HadCM3 and UKMO-HadGEM; see Randall *et al.* [19] for a full description of the climate models.

For both ensembles, each GCM is assumed to be an equally plausible projection and no model weighting or transformation of the ensemble outputs into a probability distribution has been applied.

A +4°C world is defined here as a one where a GCM's decadal global mean temperature is +4°C warmer than the 1961–1990 average in at least one season. This is different from the standard UNFCCC definitions for global warming, which are relative to pre-industrial temperatures; assuming a global warming of *ca* 0.7°C since 1850, our +4°C world is about 4.7°C warmer than pre-industrial. We select models that show an increase in global mean temperature of 2°C and 4°C at some point in the twenty-first century. For the CPDN simulations, this results in an ensemble of 1518 and 399 members for the +2°C and +4°C worlds, respectively. For the CMIP3 ensemble, all models exhibit a 2°C warming at some point in the twenty-first century, but only one model, namely MIROC3.2 (hires), warms by 4°C by 2100.

(*b*) *The climate variables*

The global hydrological model we use requires monthly inputs of precipitation and number of rain days, as well as several variables needed to determine potential evapotranspiration: temperature, vapour pressure, radiation and wind speed. These are available for the present day from the CRU TS2.1, 0.5° latitude/longitude observed climate dataset [20], where we use the time period 1961–1990 as our 'baseline' against which future changes are assessed, but regridded to 1° latitude/longitude, the resolution of the hydrological model.

As the CPDN experiment relies on distributed computing, where members of the public run a GCM on their personal computers [14], bandwidth limitations mean that only limited numbers of diagnostics are returned to the CPDN servers for archiving. Of the input variables needed for the

hydrological model, only precipitation and temperature are available, as decadal seasonal means and at the model native resolution of 3.75° longitude by 2.5° latitude.

Climate models are well known to contain biases in their climatology; for precipitation especially, any large biases can force the hydrological model to operate outside the range of the parametrizations that are used to simulate surface run-off. To correct for these biases, we use the change factor method whereby absolute changes in temperature and percentage changes in precipitation fields from a GCM for a 30 year period (e.g. 2000–2029) are calculated relative to a 1961–1990 baseline. The seasonal change factors were then disaggregated linearly to produce monthly factors, and interpolated to a 1° latitude/longitude resolution, as required by the hydrological model. To calculate future climate, precipitation and temperature change factors are then applied to the CRU TS2.1 baseline climate; other climate variables required by the hydrological model, for which we do not have GCM data, were kept the same as observed climate. One of the main criticisms of this bias-correction method is that it only adjusts the long-term mean and does not take into account additional changes in climate variability [21]. However, given that only decadal seasonal means are available from CPDN, a more sophisticated method of downscaling would not be warranted. The CMIP3 GCMs were processed in an identical manner to allow direct comparisons in the analysis.

(*c*) *Water availability*

(i) *Global hydrological model*

We employ the MacPDM global hydrological model at a 1° spatial resolution. MacPDM is a semi-distributed daily water balance model that has been used in previous assessments of global water resources [7–9,22,23], and at its heart is a simplified version of the probability distribution model by Moore [24]. The model contains modules that simulate snowpack, lakes and wetlands but does not include a glacier component. As well as climate variables, other inputs include land cover, which has been derived from De Fries *et al.* [25], and soil textures, which have been taken from the FAO Digital Soil Map of the World. MacPDM internally disaggregates monthly precipitation to daily rates by using information on the number of rain days in each month and a random precipitation generator. The model is then run 10 times and the mean of the model outputs used. MacPDM outputs surface run-off at the monthly time step that, for this study, has been aggregated to mean seasonal values to reflect the temporal resolution of the CPDN climate model ensemble.

There are a large number of global hydrological models, including those currently involved in the WATCH project [26], some of which treat the hydrological system in a more sophisticated manner than MacPDM. However, MacPDM is used in this investigation owing to its relative simplicity and therefore amenability for running large ensembles. The spatial resolution used in this study is also not as fine as those used by others [5–11] but does compare well with recently published work [27–29]. Despite infrastructure and flow routing not being included in the model, the compromise in the spatial resolution should not hinder our analysis of impacts on a larger, more synoptic scale.

(ii) *Water stress index*

Water stress or scarcity can be defined as the balance between water supply (potential or realized) and water demand. A large number of water stress indices have been devised, incorporating information on factors such as accessibility of water under low flow conditions (e.g. [30]), water demands with the inclusion of national water withdrawal information on various water users (e.g. [11,31]), economic and technological advancement (e.g. [6,27]) as well as access to water sources (e.g. [32]). On the whole, these methodologies require a large amount of input data, much of which can be very uncertain. Given that the main purpose of this paper is to look at the impacts of two global temperature regimes by using large climate model ensembles, we have chosen to analyse the water resources *per capita* calculated as the ratio of annual surface run-off to population, which we call here the water stress index (WSI). Although simple and rather limited in its reflection of true water stress [33], it provides a less complicated view rather than having to attempt to tease information out from a more sophisticated WSI.

The annual surface run-off required for the baseline WSI was obtained by driving MacPDM using the observed climate dataset for 1961–1990. The baseline population was obtained by using the Gridded Population of the World version 3 (GPWv3) dataset for 1990 [34] at a 1° resolution.

To calculate future WSI, we develop scenarios for future population growth for the 2030s and 2060s based on UN Population Division projections [35]. These projections are available at the national scale and provide estimates for urban and rural population growth up to 2050. As the GPWv3 is only available up to 2015, we have used a 30″ dataset that defines urban areas (also included in the GPWv3 [36]) to determine the spatial distribution of rural and urban populations. The UN rural and urban growth projections were applied to the baseline population according to country and whether they are rural or urban cells (a procedure similar to that of Gaffin *et al.* [37]). Finally, the populations were aggregated to a 1° spatial resolution. We have used the medium variant only for population growth and, as UN population growth rate projections are only available up to 2050, linear extrapolation was used to calculate the population for the 2060s for each country.

3. Results

(*a*) *Present-day water availability*

The baseline climatology of 1961–1990, representing the present-day climate, was used to drive MacPDM, producing monthly surface run-off values which were then aggregated to mean annual and seasonal values. The results of the baseline run are presented in figure 1*b*, representing the mean annual surface run-off (MAR) for the baseline time horizon. At this scale, a qualitative assessment of the spatial distribution of MAR reveals a similar pattern to that of mean annual precipitation (MAP; figure 1*a*), reflecting the strong control of precipitation on the water balance. Greenland has been excluded from this analysis as simple gridded hydrological models are notoriously bad at being able to capture the hydrology of the area. Further, from a water resource perspective, Greenland is not of particular significance.

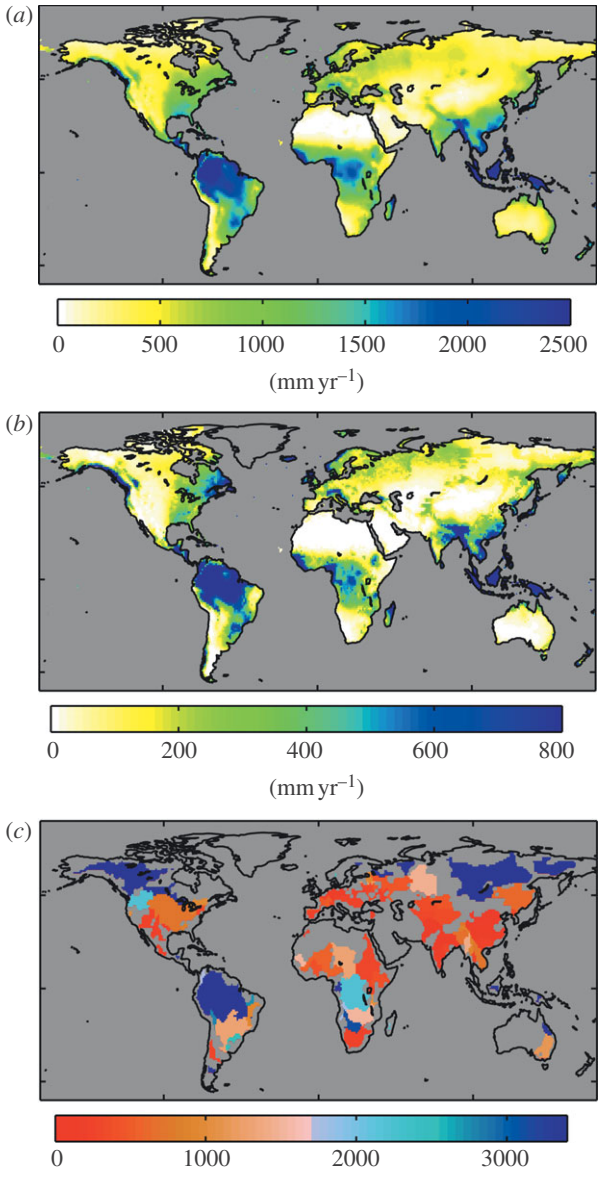

Figure 1. (*a*) Global mean annual precipitation, (*b*) mean annual surface run-off and (*c*) river basin WSI for the baseline period (1961–1990).

Total MAR and total population have been calculated and used to compute the WSI for 112 large river basins across the globe for the baseline period (figure 1*c*). The cells have been aggregated to the river basin level as a cell-by-cell analysis of the WSI would distort the results and represent a highly water-stressed world as transfers and reallocation of water by rivers, canals or pipelines from one part of a river basin to another would be ignored [9]. The WSI can be converted into the popular Falkenmark stress indicator where populations showing water availability

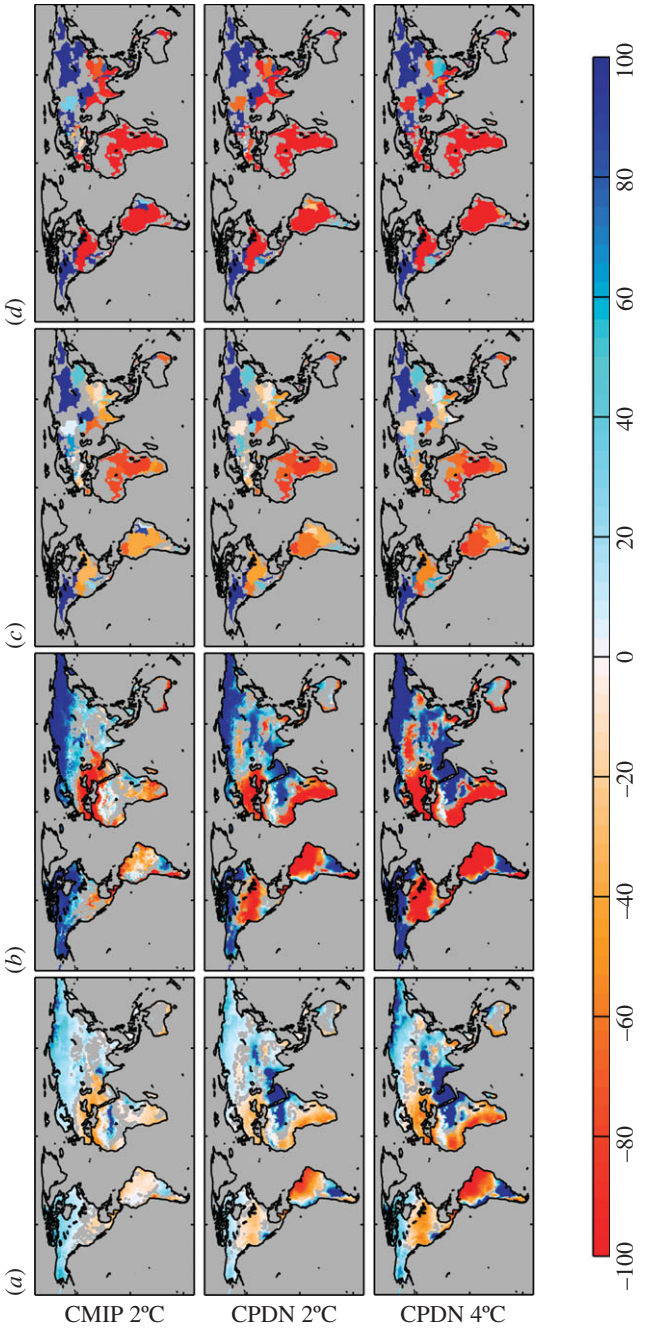

Figure 2. (*a*) Spatial pattern of ensemble-average changes in mean annual run-off (ΔMAR), (*b*) model consensus on direction of change in run-off, (*c*) ensemble-average change in water stress (ΔWSI) and (*d*) model consensus on the direction of change in water stress for a 2°C and 4°C rise in temperature and UNPOP60 population scenario compared with the baseline period. For the model consensus, red and therefore negative values represent the percentage of models showing a negative change in the respective parameter and for blue, positive values, represent the percentage of models showing a positive change. For ΔMAR and ΔWSI, colour classification spans from −100% to greater than 100% (this means that high positive values of ΔMAR and ΔWSI are effectively filtered out in these plots), whereas for consensus, colour classification spans from −100% to 100%. For plots of ΔMAR and consensus for the direction of change in run-off, grey land areas represent where ΔMAR is less than natural variability. For ΔWSI and consensus for direction of change in water stress, only 112 major river basins are plotted (Greenland has been excluded from the analysis).

under 1700 m^3 *per capita* per year are classified as being water stressed [38] and the colour scale of figure 1*c* has been devised accordingly whereby any areas showing a value of WSI less than 1700 m^3 *per capita* per year are coloured from pink to red and those showing a greater value, i.e. no stress, from pale to dark blue. According to the Falkenmark stress indicator, the WSI shows that many of the world's large river basins are currently showing signs of extreme water stress, including those in South Asia, Southeast Asia, the Nile and eastern USA, i.e. in regions of the world where there are large populations.

(*b*) *Future water availability*

(i) *Global mean annual surface run-off and model consensus*

We now analyse the spatial distribution of the change in MAR (ΔMAR), change in WSI (ΔWSI) and the consensus among the MME and PPE ensembles for a +2°C and +4°C world. As the CMIP3 ensemble only contains one member that reaches a 4°C warming, we do not include an analysis of this ensemble at 4°C. For MAR, we only show the mean of ensemble members that show changes greater than natural variability: this has been defined as twice the standard deviation of the 30 year average annual run-off in the baseline period. If we compare the +2°C and +4°C worlds of the CPDN ensemble, it is clear that ΔMAR (figure 2*a*) becomes larger in the latter, as areas previously showing changes smaller than natural variability become more noticeable. We also evaluate consensus across the ensembles, defined as the percentage of models that show the same direction of change (figure 2*b*). The consensus is an indication of the uncertainty of the projected MAR where a smaller percentage value represents areas where there is little agreement on the direction of change in the ensemble and vice versa. Note that we only show areas of consensus where ΔMAR is larger than natural variability. In the +4°C world, there is stronger model consensus in many parts of the world and the spatial extent of these areas becomes larger. This result agrees partly with that of Milly *et al.* [5] who showed that regions experiencing a decrease in run-off are projected to grow in magnitude and spatial extent. For each ensemble member, we calculated the correlation between ΔMAR at corresponding gridpoints at +2°C and +4°C. Across the CPDN ensemble, there is a high correlation[1] between areas that get drier/wetter in the two temperature regimes, i.e. the pattern of changes in MAR at +2°C and +4°C is consistent in the direction of change, but amplified at +4°C. Thus, the ensemble shows linearity of hydrological response in relation to temperature: an assumption that underlies many of the pattern-scaling-based downscaling procedures for impact assessments [21].

A comparison of the CMIP3 and CPDN ensembles at +2°C shows that there is reasonable agreement in most parts of the world for the direction of ΔMAR apart from an area encompassing eastern Africa and the Middle East. For the CPDN ensemble, the positive direction of change in MAR in eastern Africa agrees with HadCM3, the GCM on which the CPDN is based (not shown). However, the positive changes in the Middle East, which are greater than that of natural variability, are not seen in HadCM3 where changes are either smaller than natural variability or negative. Figure 2 shows that there is much stronger consensus in

[1]Ninety per cent of the ensemble members have a correlation between 0.87 and 0.97.

many regions of the world for the CPDN ensemble compared with the CMIP3 ensemble, most likely owing to the fact that the CPDN ensemble is based only on one GCM, albeit with a wide range of physics parameter values.

We also explored the relative importance of changes in precipitation and evaporation on MAR, although completely disentangling the two effects is difficult without additional experiments. In our simulations, changes in potential evaporation (PE) are a function of temperature change only, as we assume other variables are unchanged in the future. Actual evaporation (AE) is dependent on both PE and soil water availability, so that in areas where there is soil water stress, increases in PE will not translate into equivalent changes in AE. For global land areas, the average ratio of MAR to MAP decreases in all simulations as one moves from the present day to +2°C and +4°C worlds (not shown), indicating that AE increases as a proportion of the overall water balance. However, this relative proportion also varies according to the direction and extent of precipitation change, with the ensemble members with the greatest reductions in precipitation showing the smallest decreases in MAR : MAP. This effect is amplified in a +4°C world, so that ensemble members that are particularly dry do not show as large a reduction in MAR : MAP going from +2°C to +4°C as they do going from the present to +2°C.

(ii) *Global water stress index and model consensus*

The mean percentage changes in WSI compared with the baseline WSI for the major river basins of the world across each of the climate model ensembles are also shown in figure 2, for the 2060s population scenario. Similar patterns to those found for ΔMAR emerge as one moves from the present day to +2°C and +4°C worlds, with 71 and 74 per cent of the basins showing an ensemble mean increase in stress (decrease in WSI) at +2°C and +4°C, respectively. For river basins that show an increase in stress, the stressed areas generally grow in spatial extent and magnitude as one moves from +2°C to +4°C, with 71 per cent of basins becoming *more* stressed.

A number of rivers show a different sign of change for WSI at +2°C and +4°C. The Godavari, Tapti and Yangtze basins show a decrease in WSI in a +2°C world and an increase in WSI in a +4°C world; the opposite trend occurs for Dniester, Garonne, Oder, Vistula, Rio Grande de Santiago, Sacramento and Chubut basins. The change in population and the directions of change in run-off in these basins for both temperature regimes are in fact the same: it is the magnitude of the changes in run-off and population that results in the opposite signs of change in WSI for the two temperature regimes. For the first set of basins, the changes in run-off are small and close to natural variability in a +2°C world. An increase in the population is observed for the 2060s, hence there is an increase in stress. However, in the +4°C world, the increase in run-off is much larger, thereby showing a decrease in stress. The reverse is observed for the second set of basins.

The CMIP3 and CPDN ensembles for the +2°C world are in general agreement that water stress will increase in all river basins in Africa, India, eastern USA and southern Europe; these areas are regions that are already indicated as experiencing some water stress for the baseline period according to the Falkenmark stress indicator (figure 1*c*).

Consensus for WSI across each ensemble (figure 2*d*) is stronger than for MAR. This suggests that for the majority of river basins, the direction of change in WSI is very much dependent on the population in the basin, at least for the 2060s population scenario, i.e. depending on the basin, the population numbers are more important in determining the change in WSI than the spread of values across the climate ensembles. In fact, for 64 per cent of the river basins driven by the CPDN ensemble, there is greater than 99 per cent consensus in the direction of change in WSI for both temperature regimes. This also follows for the CMIP3 ensemble where 74 per cent of the ensemble shows consensus in the direction of change in WSI for the +2°C world. However, in a small number of river basins, there is little consensus at either +2°C or +4°C. For this subset of river basins (where consensus is less than 50%), we have compared ΔWSI for both the 2030s and 2060s population scenarios (not shown here). We find that there is no consistent signal in the change in consensus in WSI, for the two population scenarios, indicating that it is the uncertainty in the climate that dominates ΔWSI in these particular basins.

(iii) *River basins*

We next examine in more detail water resource response to climate model projections at +2°C and +4°C by focusing on six major river basins: the Amazon, Danube, Ganges, Mississippi, Murray Darling and Nile. In figure 3, we have plotted the frequency distributions for ΔMAR and ΔWSI for a 2°C and a 4°C warming for the CPDN ensemble for each basin. The response in the CMIP3 ensemble at +2°C has also been included, but because of the smaller size of this ensemble, we represent each ensemble member individually.

Once again, the ΔMAR frequency distributions for each of the river basins confirm the finding that ΔMAR in a +2°C world is amplified in a +4°C world. In particular, in a number of the basins, the entire frequency distribution for CPDN at +4°C becomes distinct from present-day MAR. However, the magnitude of these changes and differences between the CPDN and CMIP3 ensembles are dependent on the river basin analysed. For the Ganges, Amazon and Mississippi basins, the signal for ΔMAR for the CPDN ensemble in both the +2°C and +4°C worlds does not cover the range of ΔMAR values for the CMIP3 ensemble in a +2°C world. The Ganges and Amazon basins have already been identified here, and in the IPCC AR4, as areas where there is little consensus across the CMIP3 ensemble and great uncertainty exists in future projections of precipitation change. Thus, despite the stronger consensus shown by the CPDN ensemble for these regions, the ΔMAR values for the CMIP3 ensemble demonstrate the need to analyse an MME to capture the range of possible projections of ΔMAR.

An additional subset of climate models has also been plotted in figure 3, comprising those models that show a warming of 4°C, but at the point they warm to 2°C. While the range of this subset lies within that of the range for the full +2°C ensemble, the shapes of both frequency distributions are very similar. This suggests that the +4°C ensemble, although smaller in size, is representative of the responses that might be expected were the CPDN simulations long enough to allow all members to warm by 4°C. A spatial correlation analysis of the changes in run-off between all 1538 models showing a 2°C warming and all 339 models showing a 4°C warming run-off shows that over 50 per cent of the models have

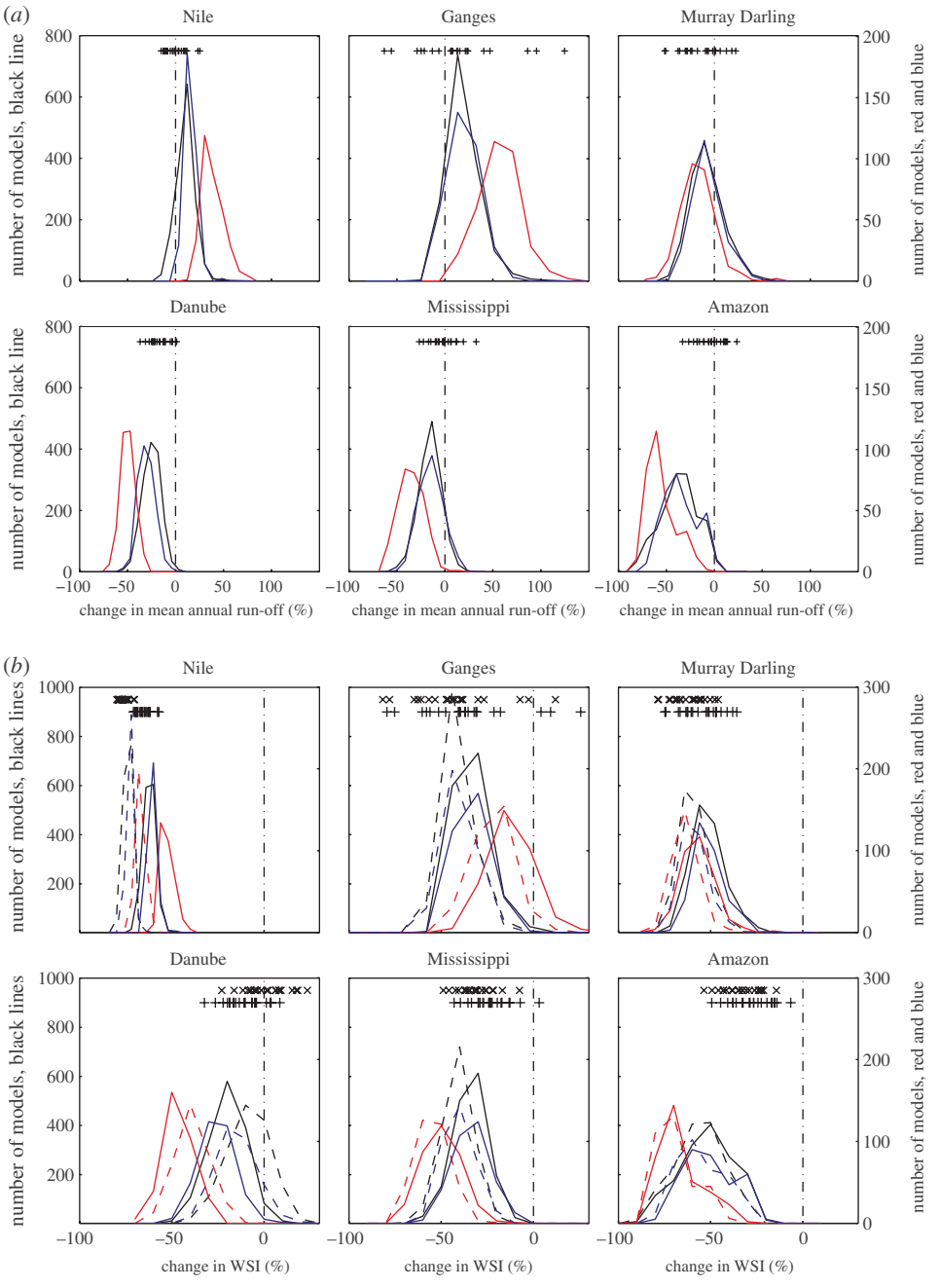

Figure 3. Changes in (*a*) MAR and (*b*) WSI for a +2°C and +4°C world for large river basins: Nile, Ganges, Murray Darling, Danube, Mississippi and Amazon, where frequency distributions are for CPDN models and pluses or crosses represent each CMIP model for a +2°C or +4°C world, respectively. Solid lines represent population scenario UNPOP2030 and dashed lines UNPOP2060. Black lines are for models that show a 2°C warming, red lines for a 4°C warming and blue lines for models in a +2°C world that show a +4°C warming at some point in the twenty-first century.

a correlation coefficient of 0.90, i.e. for a large proportion of the world's land surface, there is a clear linear relationship between run-off and the two global temperature regimes. This should also be compared with the spatial correlation of the respective annual precipitation fields, where the correlation appears to be weaker where 50 per cent of the models have a correlation coefficient of at least 0.742.

We next turn to the WSI, and here we look at how stress varies under both the 2030s and 2060s population scenarios (figure 3*b*). In each basin, changes in demand produce a complex set of possible futures. For the Danube basin, population is projected to decrease and although most of the models for the two temperature regimes show increased stress for the 2030s, driven by run-off decreases, by the 2060s, some ensemble members produce decreased stress. Thus, the direction of change here is finely balanced between projected ΔMAR and population as we move between the different global temperature regimes and population scenarios. The Murray Darling experiences a large increase in stress, which may be a surprising result for a country such as Australia, where low growth projections would be expected. However, as the Murray Darling contains large urban centres and urbanization is projected to increase through the twenty-first century, there is a corresponding large projected increase in population in the Murray Darling. This leads to an amplification of stress related to reduced MAR, and more than offsets the effects in ensemble members where MAR is projected to increase.

Two of the selected basins show increases in ΔMAR, namely the Ganges and the Nile, but while the Nile experiences increases in water stress, for all climate and population scenarios, a large number of the CPDN ensemble shows decreases in water stress for a +4°C world under both population scenarios for the Ganges. Thus, as one moves from +2°C to +4°C, the effects of climate change become large enough to offset the large increases in demand expected in the Ganges basin.

For the Ganges basin, the CMIP3 ensemble shows not only a wider range of changes in MAR and WSI than the CPDN ensemble for a 2°C warming but also contains some members that are situated in the extreme wet end of the CPDN ensemble for a 4°C warming. For the Amazon basin, the CPDN ensemble is biased towards a drier future (consistent with the findings of Li *et al.* [39] for HadCM3) and the CMIP3 ensemble, while consistently dry, is not as extreme. It should be reiterated here that the two climate ensembles used here have different purposes: the PPE is used to explore parametric uncertainties in climate models, whereas the MME for structural uncertainties in climate models. The spread of ΔMAR and ΔWSI shown here highlights the necessity of using both ensembles to capture the range of climate futures.

(iv) *Seasonality of changes*

For some river basins where there is little in the form of natural or man-made water storage to smooth out the changes in run-off throughout the hydrological year, the seasonality of the water availability is of paramount importance. To look at this, the change in seasonal run-off has been assessed (figure 4). For all river basins, apart from the Amazon, the seasonality of run-off becomes stronger as one moves from a +2°C to a +4°C world, with wet seasons becoming wetter

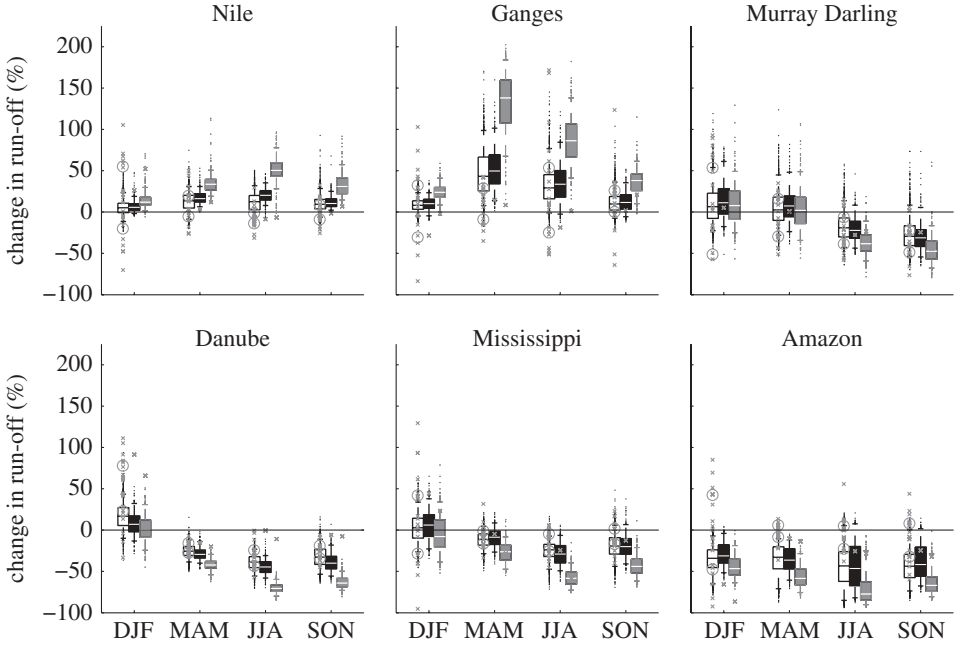

Figure 4. Seasonal changes in MAR for large river basins for CPDN ensemble, where top, middle and bottom of boxes represent 25th, 50th and 75th percentiles, respectively, whiskers extend to 5th and 95th percentiles and dots represent outliers: white boxes are for models that show a 2°C warming, black boxes are for a 4°C warming and grey boxes are for models in a +2°C world that show a 4°C warming at some point in the twenty-first century. Members of the CMIP3 ensemble are represented as crosses and the corresponding 25th and 75th percentiles marked with circles.

and dry seasons becoming drier. Given that the Amazon is largely tropical, and spans the seasonal migration of the inter-tropical convergence zone, there is little change in the seasonal regime for both +2°C and +4°C temperature regimes.

If changes in annual average stress are considered, as in figure 3, it would appear that stress in the Ganges and Nile will decrease as climate change progresses. However, figure 4 shows that the increase in surface run-off may be unevenly distributed across the year, and unless storage is available to smooth out the peaks in water availability throughout the year, the greater run-off volumes may present more difficulties, e.g. flooding, rather than alleviating water stress. However, it must be noted that GCMs find it notoriously difficult to model the Indian monsoon, so the results for the Ganges should be treated with particular caution [40]. Figure 4 also shows that the ensemble spread appears to be consistent for some basins as one moves from a +2°C world to a +4°C world, although the spread appears to be less for the Amazon and greater for the Ganges at +4°C.

4. Discussion

Through the use of a large PPE, we have shown that changes in mean annual run-off in a +2°C world are generally amplified in a +4°C world: drier areas dry further and wetter areas become wetter. Moreover, as these changes in MAR

become amplified, both the consensus and spatial coherence of these changes strengthen. By investigating the changes in water stress in 112 of the world's major river basins, we have also found that the majority of these river basins are projected to suffer greater water stress in a +4°C world than in a +2°C world. However, as we move from a +2°C to a +4°C world, there are also a small but increasing number of basins that may experience less water stress, as they are located in regions where rainfall is projected to increase.

By using population growth scenarios for the 2030s and 2060s, we find that in a +2°C world, water stress is dominated by the change in population. However, as we move to +4°C world and the climate change signal becomes stronger, climate change can play a more dominant role in determining water stress in a river basin.

The timing of the global warming will be important in determining water stress across the world. Population growth is projected to increase through the twenty-first century, peaking in the middle of the century [41]. Should a rapid warming occur, with a plausible +4°C warming by the 2060s as shown by our CPDN ensemble and Betts *et al.* [42], the drier areas of the world may be affected by a combination of peak demand for water and larger decreases in run-off. However, if a more gradual warming is experienced and +4°C is reached in 2100 or beyond, when world population is projected to decline, water stress will be lower, and there will be more time to adapt to climate change.

We have also compared the PPE from the CPDN experiment and the MME from CMIP3 for a +2°C world and have shown that while there is considerable agreement between the two ensembles, there are significant regional differences as well. Thus, in order to capture the range of possible projections, both sets of climate model ensembles are required.

By examining a subset of the world's major river basins, we have shown that the picture for water stress in each river basin is dependent on the magnitude of the climate change and the nature of the population growth. For some river basins, the effects of climate change become large enough to offset the large increases in demand in a +4°C world, e.g. in the Ganges; in most basins, however, climate and population growth combine to increase stress or climate change is insufficient to offset increased demand.

We have also found that seasonality in run-off may be more pronounced in a +4°C world compared with a +2°C world; thus, even where annual average run-off increases, dry seasons can become more stressed. This could mean that more sophisticated infrastructure projects may be required in a +4°C world compared with a +2°C world in order to prevent flooding and droughts.

There are a number of caveats when interpreting our results. We have used an MME and a PPE (of one GCM) that, albeit covering a large range of climate projections, only represents a sample of the possible uncertainty range. The GCM ensembles have not been weighted or screened, recognizing that attempting to weight models is fraught with difficulty [12,13]. The bias-correction procedure used is also simplistic and does not include any information on climate variability, either inter-annual or intra-annual. Our results are therefore appropriate for assessing changes in mean run-off and stress, but not the possibility of changes in shorter term stress.

Some care must also be taken in the interpretation of the +2°C and +4°C worlds that have been used in our analysis, as the baseline used in our analysis is for the time period 1961–1990 rather than a 'pre-industrial' value or the time

period of 1980–1999 used in IPCC [43]. Mean global temperatures for 1980–1999 are warmer than for 1961–1990 by 0.16°C and may mean larger changes in both run-off and water stress for some river basins. However, if a pre-industrialized value of 1861–1890 is used, the difference is about 0.31°C cooler, with changes in future run-off and water stress smaller in some river basins than those presented in our analysis.

MacPDM has been run offline and therefore any feedbacks into the climate system have not been included. It has also not been calibrated and its parametrizations have not been explored, although previous studies on small river catchments [44,45] find that climate model uncertainty is greater than hydrological modelling uncertainty. In fact, we have found that as we move from the PPE model data (temperature and precipitation) to MacPDM output (run-off), the spatial correlation appears to increase pointing to the importance of the model input parameters, such as soil type and land cover, in controlling the resulting run-off, which may themselves change in the future owing to direct impacts of climate change, adaptation responses and CO_2 effects on plant water-use efficiency.

The calculation of PE is included within MacPDM and is based on the Penman–Monteith equation; as shown in recent studies [46,47], this could be another source of uncertainty. This issue may need to be explored in future studies to determine the sensitivity of the CPDN ensemble to the PE calculations.

The population statistics are based on only one of the UN population growth scenarios (median variant) and exploration of the uncertainty in these projections has not been carried out. These population statistics have been calculated offline and therefore, once again, no feedback effects can be carried through to the climate and hydrological models, which may be important if the spatial distribution of populations depends on the availability of water.

The WSI used in this analysis is based solely on the annual surface run-off and river basin population. It does not incorporate many of the intricacies that may exist between water-use habits, water resources management, water infrastructure and adaptative responses, to name a few, that affect on-the-ground water stress. Although simple, the WSI used in this analysis has highlighted the need to look at river basins where there is great uncertainty in the direction of change in water stress as well as the areas that show an increase in water stress. However, to start unravelling the actual change in water stress in the region, a more detailed local assessment would be required. It must also be noted here that given the GCM data that are at best decadal seasonal means, a highly detailed assessment of water resources management options for water storage in reservoirs and groundwater replenishment is beyond the scope of this analysis.

The authors would like to acknowledge Nigel Arnell for the use of the MacPDM model, the use of the UK National Grid Service for the computational resources and the funding provided by RCUK, via the Tyndall Centre for Climate Change Research. We acknowledge the modelling groups, the Programme for Climate Model Diagnosis and Intercomparison (PCMDI) and the WCRP's Working Group on Coupled Modelling (WGCM) for their roles in making available the WCRP CMIP3 multi-model dataset. Support of this dataset is provided by the Office of Science, US Department of Energy. Finally, we thank the climateprediction.net project, and the many thousands of members of the public who have donated time on their personal computers, for the climateprediction.net simulations.

References

1 UNFCCC. 2009 Copenhagen Accord. Document FCCC/CP/2009/L.7.
2 Parry, M. 2010 Copenhagen number crunch. *Nat. Rep. Clim. Change* **4**, 18–19. (doi:10.1038/climate.2010.01)
3 Sustainability Institute. 2010 Copenhagen Accord submissions press release, 4 February 2010. See http://climateinteractive.org/.
4 IPCC. 2007 *Climate change 2007: impacts, adaptation and vulnerability. Contribution of Working Group II to the 4th Assessment Report of the Intergovernmental Panel on Climate Change* (eds M. Parry, O. Canzaiani, J. Palutikof, P. van der Linden & C. Hanson), ch. 3. Cambridge, UK: Cambridge University Press.
5 Milly, P. C. D., Dunne, K. A. & Vecchia, A. V. 2005 Global pattern of trends in streamflow and water availability in a changing climate. *Nature* **438**, 347–350. (doi:10.1038/nature04312)
6 Alcamo, J., Flörke, M. & Märker, M. 2007 Future long-term changes in global water resources driven by socio-economic and climatic changes. *Hydrol. Sci. J.* **52**, 247–275. (doi:10.1623/hysj.52.2.247)
7 Arnell, N. W. 1999 Climate change and global water resources. *Glob. Environ. Change* **9**, 31–49. (doi:10.1016/S0959-3780(99)00017-5)
8 Arnell, N. W. 2003 Effects of IPCC SRES emissions scenarios on river runoff: a global perspective. *Hydrol. Earth Syst. Sci.* **7**, 619–641. (doi:10.5194/hess-7-619-2003)
9 Arnell, N. W. 2004 Climate change and global water resources: SRES emissions and socio-economic scenarios. *Glob. Environ. Change* **14**, 31–52. (doi:10.1016/j.gloenvcha.2003.10.006)
10 Kundzewicz, Z. W., Mata, L. J., Arnell, N. W., Doll, P., Jimenez, B., Miller, K., Oki, T., Sen, Z. & Shiklomanov, I. 2008 The implications of projected climate change for freshwater resources and their management. *Hydrol. Sci. J.* **53**, 3–10. (doi:10.1623/hysj.53.1.3)
11 Vörösmarty, C. J. 2000 Global water resources: vulnerability from climate change and population growth. *Science* **289**, 284–288. (doi:10.1126/science.289.5477.284)
12 Knutti, R. 2008 Should we believe model predictions of future climate change? *Phil. Trans. R. Soc. A* **366**, 4647–4664. (doi:10.1098/rsta.2008.0169)
13 Tebaldi, C. & Knutti, R. 2007 The use of the multi-model ensemble in probabilistic climate projections. *Phil. Trans. R. Soc. A* **365**, 2053–2075. (doi:10.1098/rsta.2007.2076)
14 Allen, M. R. 1999 Do-it-yourself climate prediction. *Nature* **401**, 642. (doi:10.1038/44266)
15 Meehl, G. A., Covey, C., Delworth, T., Latif, M., McAvaney, B., Mitchell, J. F. B., Stouffer, R. J. & Taylor, K. E. 2007 The WCRP CMIP3 multimodel dataset. *Bull. Am. Meteorol. Soc.* **88**, 1383–1394. (doi:10.1175/BAMS-88-9-1383)
16 Allen, M. R. & Stainforth, D. A. 2002 Towards objective probabilistic climate forecasting. *Nature* **419**, 228. (doi:10.1038/nature01092a)
17 Stainforth, D. A. *et al.* 2005 Uncertainty in predictions of the climate response to rising levels of greenhouse gases. *Nature* **433**, 403–406. (doi:10.1038/nature03301)
18 Nakićenović, N. C. 2000 *Special report on emissions scenarios: a special report of Working Group III of the Intergovernmental Panel on Climate Change*. Cambridge, UK: Cambridge University Press.
19 Randall, D. A. *et al.* 2007 Climate models and their evaluation. In *Climate change 2007: the physical science basis* (eds S. Solomon, D. Qin, M. Manning, M. Marquis, K. Averyt, M. M. B. Tignor, H. L. Miller & Z. Chen), pp. 589–662. Cambridge, UK: Cambridge University Press.
20 Mitchell, T. D. & Jones, P. D. 2005 An improved method of constructing a database of monthly climate observations and associated high-resolution grids. *Int. J. Climatol.* **25**, 693–712. (doi:10.1002/joc.1181)
21 Xu, C. Y. 1999 From GCMs to river flow: a review of downscaling methods and hydrologic modelling approaches. *Prog. Phys. Geogr.* **23**, 229–249. (doi:10.1177/030913339902300204)
22 Arnell, N. W. 1999 A simple water balance model for the simulation of streamflow over a large geographic domain. *J. Hydrol.* **217**, 314–335. (doi:10.1016/S0022-1694(99)00023-2)
23 Arnell, N. W. & Delaney, E. K. 2006 Adapting to climate change: public water supply in England and Wales. *Clim. Change* **78**, 227–255. (doi:10.1007/s10584-006-9067-9)

24 Moore, R. J. 2007 The PDM rainfall-runoff model. *Hydrol. Earth Syst. Sci.* **11**, 483–499. (doi:10.5194/hess-11-483-2007)

25 De Fries, S., Hansen, M. & Town, J. G. R. 1998 Global land cover classifications at 8 km spatial resolution: the use of training data derived from Landsat imagery in decision tree classifiers. *Int. J. Remote Sens.* **19**, 3141–3168. (doi:10.1080/014311698214235)

26 Haddeland, I. D. *et al.* Submitted. Multi-model estimate of the global water balance: setup and first results.

27 Hanasaki, N., Kanae, S., Oki, T., Masuda, K., Motoya, K., Shirakawa, N., Shen, Y. & Tanaka, K. 2008 An integrated model for the assessment of global water resources—part 2: applications and assessments. *Hydrol. Earth Syst. Sci.* **12**, 1027–1037. (doi:10.5194/hess-12-1027-2008)

28 Oki, T. 2006 Global hydrological cycles and world water resources. *Science* **313**, 1068–1072. (doi:10.1126/science.1128845)

29 Oki, T., Agata, Y., Kanae, S., Saruhashi, T., Yang, D. & Musiake, K. 2001 Global assessment of current water resources using total runoff integrating pathways. *Hydrol. Sci. J.* **46**, 983–996. (doi:10.1080/02626660109492890)

30 Meigh, J. R., McKenzie, A. A. & Sene, K. J. 1999 A grid-based approach to water scarcity estimates for eastern and southern Africa. *Water Resour. Manage.* **13**, 85–115. (doi:10.1023/A:1008025703712)

31 Shiklomanov, I. A. 2000 Appraisal and assessment of world water resources. *Water Int.* **25**, 11–32. (doi:10.1080/02508060008686794)

32 Sullivan, C. A. & Meigh, J. 2007 Integration of the biophysical and social sciences using an indicator approach: addressing water problems at different scales. *Water Resour. Manage.* **21**, 111–128. (doi:10.1007/s11269-006-9044-0)

33 Rijsberman, F. R. 2006 Water scarcity: fact or fiction? *Agric. Water Manage.* **80**, 5–22. (doi:10.1016/j.agwat.2005.07.001)

34 CIESIN, CIAT. 2005 Gridded population of the world version 3 (GPWV3): population density grids. Technical report, Center for International Earth Science Information Network (CIESIN), Socioeconomic Data and Applications Center (SEDAC), Columbia University, Palisade, NY, USA. See http://sedac.ciesin.columbia.edu/gpw.

35 DESA. 2007 World population prospects: the 2006 revision and world urbanization prospects: the 2007 revision. Technical report, Population Division of the Department of Economic and Social Affairs of the United Nations Secretariat, New York, USA.

36 CIESIN, IFPRI, World Bank, CIAT. 2004 Global rural-urban mapping project (GRUMP), alpha version: urban extents. Technical report, Center for International Earth Science Information Network (CIESIN), Columbia University; International Food Policy Research Institute (IFPRI); The World Bank; and Centro Internacional de Agricultura Tropical (CIAT), Socioeconomic Data and Applications Center (SEDAC), Columbia University, Palisades, NY, USA. See http://sedac.ciesin.columbia.edu/gpw.

37 Gaffin, S. R., Rosenzweig, C., Xing, X. & Yetman, G. 2004 Downscaling and geo-spatial gridding of socio-economic projections from the IPCC Special Report on Emissions Scenarios (SRES). *Glob. Environ. Change* **14**, 105–123. (doi:10.1016/j.gloenvcha.2004.02.004)

38 Falkenmark, M., Lundqvist, J. & Widstrand, C. 1989 Macro-scale water scarcity requires micro-scale approaches. *Nat. Resour. Forum* **13**, 258–267. (doi:10.1111/j.1477-8947.1989.tb00348.x)

39 Li, W., Fu, R. & Dickinson, R. E. 2006 Rainfall and its seasonality over the Amazon in the 21st century as assessed by the coupled models for the IPCC AR4. *J. Geophys. Res.* **111**, D02111. (doi:10.1029/2005JD006355)

40 Turner, A. G. & Slingo, J. M. 2009 Uncertainties in future projections of extreme precipitation in the Indian monsoon region. *Atmos. Sci. Lett.* **10**, 152–158. (doi:10.1002/asl.223)

41 Lutz, W., Sanderson, W. & Scherbov, S. 2008 IIASA's 2007 probabilistic world population projections. IIASA World Population Program Online Data Base of Results 2008. See http://www.iiasa.ac.at/Research/POP/proj07/index.html?sb=5.

42 Betts, R. A., Collins, M., Hemming, D. L., Jones, C. D., Lowe, J. A. & Sanderson, M. G. 2011 When could global warming reach 4°C? *Phil. Trans. R. Soc. A* **369**, 67–84. (doi:10.1098/rsta.2010.0292)

43 IPCC. 2007 *Climate change 2007: the physical science basis. Contribution of Working Group I to the 4th Assessment Report of the Intergovernmental Panel on Climate Change* (eds S. Solomon, D. Qin, M. Manning, Z. Chen, M. Marquis, K. B. Averyt, M. Tignor & H. L. Miller), ch. TS.5. Cambridge, UK: Cambridge University Press.

44 New, M., Lopez, A., Dessai, S. & Wilby, R. 2007 Challenges in using probabilistic climate change information for impact assessments: an example from the water sector. *Phil. Trans. R. Soc. A* **365**, 2117–2131. (doi:10.1098/rsta.2007.2080)

45 Wilby, R. L. 2005 Uncertainty in water resource model parameters used for climate change impact assessment. *Hydrol. Process.* **19**, 3201–3219. (doi:10.1002/hyp.5819)

46 Kay, A. L. & Davies, H. N. 2008 Calculating potential evaporation from climate model data: a source of uncertainty for hydrological climate change impacts. *J. Hydrol.* **358**, 221–239. (doi:10.1016/j.jhydrol.2008.06.005)

47 Kingston, D. G., Todd, M. C., Taylor, R. G., Thompson, J. R. & Arnell, N. W. 2009 Uncertainty in the estimation of potential evapotranspiration under climate change. *Geophys. Res. Lett.* **36**, L20403. (doi:10.1029/2009GL040267)